

Comparison of $p + A$ and Si + Au Collisions at 14.6 GeV/c

T. Abbott,⁽⁴⁾ Y. Akiba,⁽⁷⁾ D. Beavis,⁽²⁾ M. A. Bloomer,^{(10),(a)} P. D. Bond,⁽²⁾ C. Chasman,⁽²⁾ Z. Chen,⁽²⁾ Y. Y. Chu,⁽²⁾ B. A. Cole,⁽¹⁰⁾ J. B. Costales,^{(10),(b)} H. J. Crawford,⁽³⁾ J. B. Cumming,⁽²⁾ R. Debbe,⁽²⁾ J. Engelage,^{(3),(9)} S. Y. Fung,⁽⁴⁾ L. Grodzins,⁽¹⁰⁾ S. Gushue,⁽²⁾ H. Hamagaki,⁽⁷⁾ O. Hansen,⁽²⁾ R. S. Hayano,⁽¹¹⁾ S. Hayashi,^{(7),(c)} S. Homma,⁽⁷⁾ H. Z. Huang,^{(10),(a)} Y. Ikeda,^{(8),(d)} I. Juricic,⁽⁵⁾ J. Kang,⁽⁴⁾ S. Katcoff,⁽²⁾ S. Kaufman,⁽¹⁾ K. Kimura,⁽⁸⁾ K. Kitamura,^{(6),(e)} K. Kurita,⁽⁵⁾ R. J. Ledoux,⁽¹⁰⁾ M. J. Levine,⁽²⁾ Y. Miake,⁽²⁾ R. J. Morse,⁽¹⁰⁾ B. Moskowitz,⁽²⁾ S. Nagamiya,⁽⁵⁾ J. Olness,⁽²⁾ C. G. Parsons,⁽¹⁰⁾ L. P. Remsberg,⁽²⁾ H. Sakurai,⁽¹¹⁾ M. Sarabura,^{(10),(f)} A. Shor,^{(2),(g)} P. Stankus,⁽⁵⁾ S. G. Steadman,⁽¹⁰⁾ G. S. F. Stephans,⁽¹⁰⁾ T. Sugitate,⁽⁶⁾ M. Tanaka,⁽²⁾ M. J. Tannenbaum,⁽²⁾ M. Torikoshi,^{(7),(h)} J. H. van Dijk,⁽²⁾ F. Videbaek,^{(1),(c)} M. Vient,^{(4),(i)} P. Vincent,^{(2),(j)} V. Vutsadakis,⁽¹⁰⁾ H. E. Wegner,⁽²⁾ D. S. Woodruff,⁽¹⁰⁾ Y. D. Wu,⁽⁵⁾ and W. Zajc⁽⁵⁾

(E802 Collaboration)

⁽¹⁾Argonne National Laboratory, Argonne, Illinois 60439-4843

⁽²⁾Brookhaven National Laboratory, Upton, New York 11973

⁽³⁾Space Sciences Laboratory, University of California, Berkeley, California 94720

⁽⁴⁾University of California, Riverside, California 92521

⁽⁵⁾Columbia University, New York, New York 10027 and Nevis Laboratories, Irvington, New York 10533

⁽⁶⁾Hiroshima University, Hiroshima 730, Japan

⁽⁷⁾Institute for Nuclear Study, University of Tokyo, Tanashi, Tokyo 188, Japan

⁽⁸⁾Kyushu University, Fukuoka 812, Japan

⁽⁹⁾Lawrence Livermore National Laboratory, Livermore, California 94550

⁽¹⁰⁾Massachusetts Institute of Technology, Cambridge, Massachusetts 02139

⁽¹¹⁾Department of Physics, University of Tokyo, Tokyo 113, Japan

(Received 19 October 1990)

The production of π^\pm, K^\pm, p has been measured in $p + \text{Be}$ and $p + \text{Au}$ collisions for comparison with central Si+Au collisions. The inverse slope parameters T_0 obtained by an exponential fit with the invariant cross sections in transverse mass are found to be $T_0^{p, K^\pm, \pi^\pm} \sim 140\text{--}160$ MeV in $p + A$ collisions, whereas in central Si+Au collisions, $T_0^{p, K^\pm} \sim 200\text{--}220$ MeV $> T_0^{\pi^\pm} \sim 140\text{--}160$ MeV at midrapidity. The π^\pm and K^\pm distributions are shifted backwards in $p + \text{Au}$ compared with $p + \text{Be}$. A gradual increase of $(dn/dy)_K$ per projectile nucleon is observed from $p + \text{Be}$ to $p + \text{Au}$ to central Si+Au collisions, while pions show no significant increase.

PACS numbers: 25.40.Ve, 25.70.Np

Relativistic heavy-ion beams available from the BNL Tandem-AGS Complex provide an opportunity for studying nuclear matter at high baryon density. The first measurements of semi-inclusive spectra of π^\pm, K^\pm , and p in central Si+Au collisions at Alternating Gradient Synchrotron (AGS) energies have been reported¹ and reveal several interesting features, among which are the following. The invariant cross sections are roughly exponential in transverse mass, with the slope for K^\pm and p flatter than for π^\pm 's, and the observed K^\pm/π^\pm ratio is considerably enhanced in central Si+Au collisions compared with the ratio observed in $p-p$ collisions.² The enhanced K^\pm/π^\pm ratio has received much attention because this can be interpreted as a signature of quark-gluon plasma.³ However, it has been also discussed in terms of thermal models^{4,5} and rescattering models.⁶⁻⁸ The systematic study of the $p + A$ reaction when compared to Si+ A may provide a method for separating these various reaction possibilities. For example, if the

K^\pm/π^\pm ratio were much larger in Si+Au than in $p + \text{Au}$, it would suggest that some kind of exotic nuclear matter had been formed. In particular, the study of the target-mass dependence of pion and kaon production in $p + A$ collisions is important for the interpretation of the large K^\pm/π^\pm ratio observed in heavy-ion experiments.¹ We report here the first measurements of particle-identified momentum spectra from proton collisions with Be and Au targets over the central rapidity region at the beam momentum of 14.6 GeV/c. Both the Si+Au experiment and this one have been performed using the E802 magnetic spectrometer for measuring momentum spectra with good particle identification. In addition, the apparatus has various event characterization detectors for the selection of charged multiplicity, neutral transverse energy, and forward energy. Details of the experimental apparatus are found in Ref. 9.

In Figs. 1(a) and 1(b) π^\pm, K^\pm , and proton spectra are shown for $p + \text{Be}$ and $p + \text{Au}$ collisions with a mini-

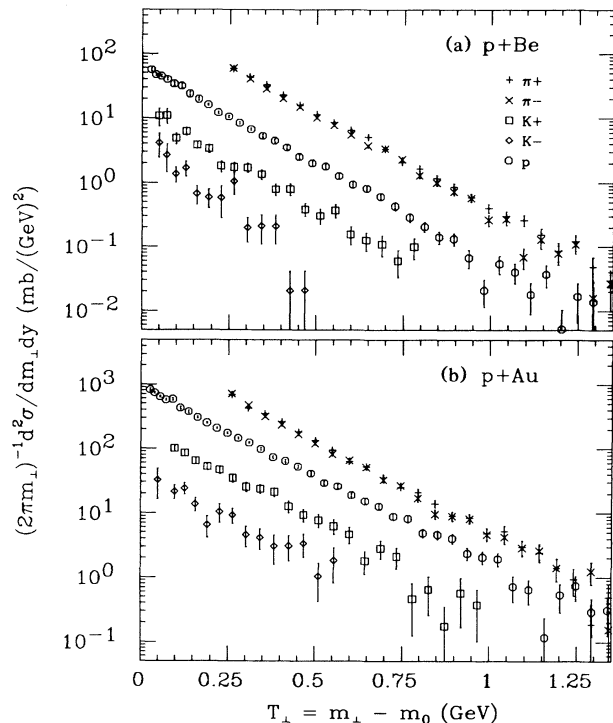


FIG. 1. Invariant cross sections as a function of $T_{\perp} = m_{\perp} - m_0$ for π^{\pm} , K^{\pm} , and protons in (a) $p + \text{Be}$ and (b) $p + \text{Au}$ collisions at the beam momentum of $14.6A \text{ GeV}/c$. The rapidity range is $1.2 \leq y \leq 1.4$ and the error bars show statistical uncertainties only. There is a $\leq 10\%$ systematic error in the absolute normalization.

mum-bias spectrometer trigger in the rapidity range $1.2 \leq y \leq 1.4$. Invariant cross sections are plotted as a function of $T_{\perp} = m_{\perp} - m_0$, where $m_{\perp} = (p_{\perp}^2 + m_0^2)^{1/2}$ is the transverse mass, p_{\perp} is the transverse momentum, and m_0 is the rest mass. Particle identification has been done by a combination of a highly segmented time-of-flight counter and a recently installed segmented-gas Čerenkov counter, which enables π and K identification up to 5 and $3.5 \text{ GeV}/c$ in the laboratory, respectively. The $p + \text{Be}$ spectra are generally consistent with previous measurements.¹⁰ As in central Si+Au collisions,¹ and also in $p-p$ collisions,² the spectra are well described as exponential in m_{\perp} . The slopes of the spectra for all particles in Fig. 1 are roughly the same, and almost constant over a wide rapidity range, $1.2 \leq y \leq 1.8$, and are also similar to those in $p-p$ collisions.² Inverse slope parameters T_0 , obtained by an exponential fit $\exp(-m_{\perp}/T_0)$ to the spectra, are shown in Fig. 2 together with those for central Si+Au collisions.¹ A clear change is seen for proton and K^+ between $p+A$ and Si+Au: In $p+A$, $T_0^{p,K^+,\pi^{\pm}} \sim 140\text{--}160 \text{ MeV}$, while in central Si+Au, $T_0^{p,K^+} \sim 200\text{--}220 \text{ MeV} > T_0^{\pi^{\pm}} \sim 140\text{--}160 \text{ MeV}$ at $1.2 \leq y \leq 1.4$. There are a variety of possible mechanisms proposed for the different slope parameters for different particle species in heavy-ion collisions, such as differences in

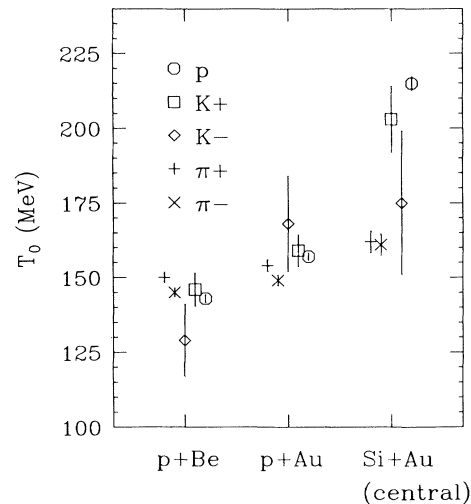


FIG. 2. Comparison of inverse slope parameters in $p + \text{Be}$, $p + \text{Au}$, and central Si+Au collisions. Inverse slope parameters are obtained by exponential fits with the invariant cross section in transverse mass. The rapidity range is $1.2 \leq y \leq 1.4$ and the error bars show statistical uncertainties only.

mean free path,¹¹ resonance decay,¹² and transverse flow.^{13,14}

By integrating the T_{\perp} spectra over the entire range of m_{\perp} with the assumption of a single exponential shape, the rapidity distributions $dn/dy = (1/\sigma_{\text{inel}}) d\sigma/dy$ are obtained. Here, σ_{inel} is the inelastic cross section with numerical values taken from Ref. 15. In Fig. 3, the dn/dy distributions per projectile nucleon are compared for $p + \text{Be}$, $p + \text{Au}$, and central Si+Au collisions. The particle identification for the central Si+Au data, which were taken before the installation of the segmented-gas Čerenkov counter, has been done solely by time of flight. This leads to its narrower rapidity coverage. The steeper component observed by E810 in the π^- spectra below the E802 acceptance, $p_{\perp} < 0.3 \text{ GeV}/c$, is claimed to contribute to an additional $\sim 25\%$ to the yield in Si+Au collisions.¹⁶ The central Si+Au data are divided by 28 because particle production per projectile nucleon provides an intuitive way to compare central Si+Au with $p+A$.^{17,18}

The shapes of the dn/dy distributions in $p + \text{Be}$ collisions are very broad for π^{\pm} and K^+ and are nearly symmetric with respect to the nucleon-nucleon center-of-mass rapidity y_{NN} , indicating that $p + \text{Be}$ collisions are roughly equivalent to $p-p$ or $p-n$ collisions. The K^- distribution in $p + \text{Be}$ shows a narrower width than the K^+ , presumably reflecting their different production mechanisms. At $y > 2$, the π^+ yield in $p + \text{Be}$ is much larger than the π^- yield, which is consistent with projectile fragmentation.

In contrast to the flat distributions for $p + \text{Be}$, the $p + \text{Au}$ distributions are not symmetric in y_{NN} but are shifted towards the target rapidity with a clear increase

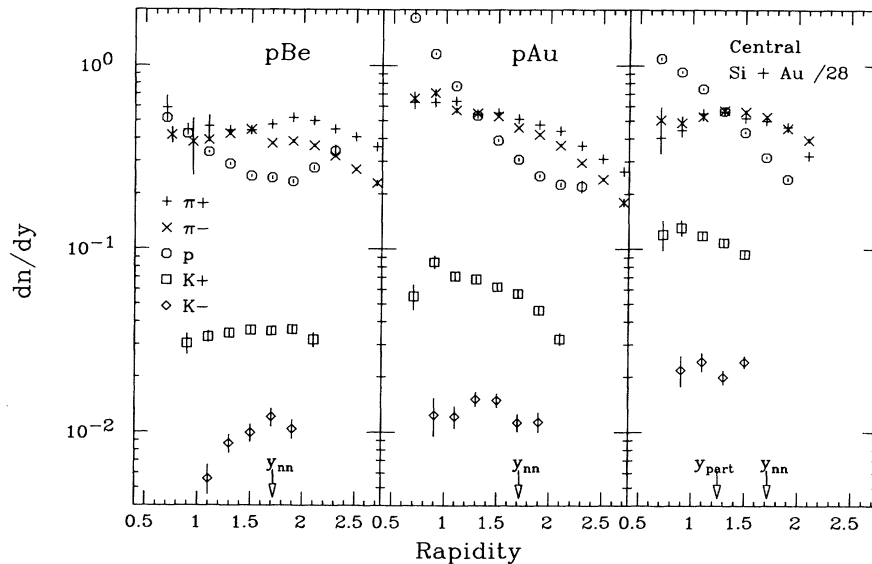


FIG. 3. Rapidity distributions dn/dy for π^\pm , K^\pm , and protons in $p+\text{Be}$, $p+\text{Au}$, and central $\text{Si}+\text{Au}$ (Refs. 1 and 20) collisions at $14.6A$ GeV/c. The central $\text{Si}+\text{Au}$ data are plotted as $(dn/dy)/28$ for comparison. The rapidity of the nucleon-nucleon center of mass, y_{NN} , and the center-of-mass rapidity for the participant nucleons, y_{part} , are also shown. The error bars show statistical uncertainties only.

in π^\pm and K^+ in the lower rapidity region. The K^- distribution is also increased and noticeably flatter. In the projectile-fragmentation region, less particle production, especially for pions, is observed in $p+\text{Au}$ compared to $p+\text{Be}$. None of these effects is seen in FRITIOF calculations,¹⁹ which give distributions that are roughly symmetric about y_{NN} for all produced particles. Consistent with isospin considerations, the yield of π^+ over π^- is greater in $p+\text{Be}$ than $p+\text{Au}$. The dn/dy distribution in $p+\text{Au}$ for protons increases very rapidly at lower rapidity, showing a mass dependence greater than A at $y \leq 1$. For the interval $y \leq 1.5$, the K^+ and protons exhibit similar target-mass dependences.

In the right panel of Fig. 3, central $\text{Si}+\text{Au}$ data^{1,20} are shown as a function of rapidity. The values of y_{NN} and y_{part} are marked on the abscissa, where y_{part} is the center-of-mass rapidity of participant nucleons, which are composed of the incident Si and a core of 75 Au nucleons swept out in zero-impact-parameter collisions. In central $\text{Si}+\text{Au}$ collisions, both π^\pm and K^+ show broad peaks, but a distinct difference is seen in their distribution shapes: While the π^\pm 's peak lies in between y_{NN} and y_{part} , the K^+ 's peak is lower than y_{part} . The backward shift in dn/dy and the flatter T_\perp slope for the K^+ distribution are strong constraints on model calculations.

The ratio of the integrated yield for $p+\text{Au}$ to $p+\text{Be}$ over the measured region ($0.6 \leq y \leq 2.6$ for pions, $0.6 \leq y \leq 2.2$ for K^+ , $0.8 \leq y \leq 2.2$ for K^- , and $0.6 \leq y \leq 2.4$ for protons) is 1.08 ± 0.03 for π^+ , 1.27 ± 0.05 for π^- , 1.81 ± 0.18 for K^+ , 1.33 ± 0.17 for K^- , and 1.95 ± 0.02 for protons. Quoted uncertainties in the present work are purely statistical. These ratios depend on the

rapidity range for the integration, because of the different distribution shapes; especially for the protons, the ratio might be considerably larger if the data extended to lower rapidity. In heavy-ion experiments at the AGS energy, it is conjectured that most projectile nucleons exhaust their energy after a few nucleon-nucleon collisions,^{17,21} which is consistent with the slow increase in pion multiplicity with increasing target size seen in the present measurements. Surprisingly, the increase of the K^+ yield with target size is markedly larger than observed for the pions and as large as for the protons.

An increase in the K^+ yield from $p+\text{Au}$ to central $\text{Si}+\text{Au}$ (divided by 28) is also seen in Fig. 3. The pion yield stays roughly the same. Therefore, the increase of the K^+/π^+ ratio²² from $p+\text{Be}$ to $p+\text{Au}$ and to central $\text{Si}+\text{Au}$ appears to originate primarily from an increase in the K^+ yield. Although the statistics are small, the K^- yield also appears to increase from $p+\text{Au}$ to central $\text{Si}+\text{Au}$ (divided by 28).

The saturation of the pion yield and the enhancement in the kaon yield imply a different production mechanism for the two species. For kaons, the increased T_0 together with the backward shift in the rapidity distributions suggests rescattering effects,⁶⁻⁸ such as multiple scattering and/or secondary production. However, if the kaons are produced in secondary reactions, then, naively, the pions, which have less mass, should be produced at least as copiously. The gradual increase of the K^+ yield from $p+\text{Be}$ to $p+\text{Au}$ and to central $\text{Si}+\text{Au}$ and the possibly enhanced K^- yield in central $\text{Si}+\text{Au}$ have been discussed as manifestations of $\pi n \rightarrow K^+\Lambda$ and $\pi n \rightarrow K^+K^-$, respectively.^{6,8} Further theoretical study is

needed to understand the data quantitatively.

As is done in Si+Au data, high-multiplicity events in $p+Au$ have been analyzed to study the effect of selecting central collisions. With high-multiplicity selection, particle production shifts more towards the target rapidity and an increase in dn/dy for K^+ is observed. However, caution is needed in comparing high-multiplicity events in $p+A$ and Si+ A . For high-multiplicity events in $p+A$ the centrality detector responds mostly to low-momentum target protons, whereas for Si+ A the detector selects events mostly on the basis of large numbers of emitted pions. Because of this difference in the definition of "centrality," the high-multiplicity $p+Au$ data require extended discussions. Nonetheless, one qualitatively interesting feature observed in $p+A$, which contrasts with Si+ A , is the lack of a significant increase in the slope parameters with selection of high-multiplicity events; $T_0^p \sim T_0^{K^+} \sim T_0^{\pi^{\pm}}$ at $1.2 \leq y \leq 1.4$. In addition, the K^+/π^+ ratios are found to lie in between those for central Si+Au and minimum-bias $p+Au$.

In conclusion, particle production of π^{\pm} , K^{\pm} , and p has been measured in $p+A$ collisions for comparison with central Si+ A collisions. The invariant cross sections are well described by an exponential in m_t with inverse slope parameters $T_0 \sim 140\text{--}160$ MeV in $p+A$ collisions. In central Si+Au collisions, T_0 is considerably higher for K^+ and protons at midrapidity. In $p+Au$ the rapidity distributions for π^{\pm} and K^+ shift towards the target rapidity, whereas in $p+Be$ they are broad and symmetric with respect to y_{NN} . A gradual increase of dn/dy for K^+ per projectile nucleon from $p+Be$ to $p+Au$ and to central Si+Au collisions is observed, while that for pions stays roughly the same. The K^+/π^+ ratio therefore shows an evolutionary increase from $p+Be$ to $p+Au$ to central Si+Au collisions at midrapidity that can be largely attributed to an increase in K^+ production.

The authors would like to thank the AGS operations staff for providing the proton beam. This work has been supported by the U.S. Department of Energy under Contracts with ANL (No. W-31-109-ENG-38), BNL (No. DE-AC02-76CH00016), Columbia University (No. DE-FG02-86-ER40281), LLNL (No. W-7405-ENG-48), MIT (No. DE-AC02-76ER03069), University of California at Riverside (No. DE-FG03-86ER40271), and NASA (No. NGR-05-003-513), under contract with the University of California, and by the U.S.-Japan High Energy Physics Collaboration Treaty.

^(a)Now at Lawrence Berkeley Laboratory, Berkeley, CA 94720.

^(b)Now at Lawrence Livermore National Laboratory, Livermore, CA 94550.

^(c)Now at Brookhaven National Laboratory, Upton, NY 11973.

^(d)Now at Hitachi Limited, Hitachi, Ibaraki 316, Japan.

^(e)Now at NTT Tsuyama, Tsuyama, Okayama 708, Japan.

^(f)Now at Los Alamos National Laboratory, Los Alamos, NM 87545.

^(g)Now at Weizmann Institute of Science, Rehovot 76100, Israel.

^(h)Now at Mitsubishi Electric Company, Hyogo 652, Japan.

⁽ⁱ⁾Now at University of California at Irvine, Irvine, CA 92717.

^(j)Now at Bruker Medical Imaging, Inc., Lisle, IL 60532.

¹E802 Collaboration, T. Abbott *et al.*, Phys. Rev. Lett. **64**, 847 (1990).

²J. V. Allaby *et al.*, CERN Report No. 70-12, 1970 (unpublished); H. Bøggild *et al.*, Nucl. Phys. **B57**, 77 (1973); D. Dekkers *et al.*, Phys. Rev. **137**, B962 (1965); U. Becker *et al.*, Phys. Rev. Lett. **37**, 1731 (1976).

³P. Koch *et al.*, Phys. Rep. **C 142**, 167 (1986); T. Matsui *et al.*, Phys. Rev. D **34**, 783 (1986); **34**, 2047 (1986).

⁴J. Cleymans *et al.*, Phys. Lett. B **242**, 111 (1990).

⁵C. M. Ko *et al.*, Phys. Rev. C **38**, 179 (1988); C. M. Ko *et al.*, Nucl. Phys. **A498**, 561c (1989).

⁶R. Mattiello *et al.*, Phys. Rev. Lett. **63**, 1459 (1989).

⁷W.-q. Chao, C.-s. Gao, and Y.-l. Zhu, Nucl. Phys. **A514**, 734 (1990).

⁸M. Gyulassy, in *Proceedings of the Workshop on Heavy Ion Physics at the AGS (HIPAGS), March 1990* (BNL Report No. BNL-44911), p. 503; C. M. Ko, *ibid.*, p. 361.

⁹E802 Collaboration, T. Abbott *et al.*, Nucl. Instrum. Methods Phys. Res., Sect. A **290**, 41 (1990).

¹⁰D. Dekkers *et al.*, Phys. Rev. **137**, B962 (1965); R. A. Lundy *et al.*, Phys. Rev. Lett. **14**, 504 (1965); J. G. Asbury *et al.*, Phys. Rev. **178**, 2086 (1969); G. M. Marmer *et al.*, Phys. Rev. **179**, 1294 (1969).

¹¹S. Nagamiya, Phys. Rev. Lett. **49**, 1383 (1982).

¹²R. Brockman *et al.*, Phys. Rev. Lett. **53**, 2012 (1984).

¹³P. J. Siemens and J. O. Rasmussen, Phys. Rev. Lett. **42**, 880 (1979).

¹⁴U. Heinz, K. S. Lee, and E. Schnedermann, in *Proceedings of the Nuclear Equation of State, Peniscola, Spain, 1989*, edited by W. Greiner and H. Spöcker (Plenum, New York, 1989), Pt. B, pp. 385-405.

¹⁵S. P. Denisov *et al.*, Nucl. Phys. **B61**, 62 (1973).

¹⁶E810 Collaboration, W. A. Love (private communication).

¹⁷E802 Collaboration, T. Abbott *et al.*, Phys. Lett. B **197**, 285 (1987).

¹⁸NA35 Collaboration, A. Bamberger *et al.*, Phys. Lett. B **184**, 271 (1987).

¹⁹B. Nilsson-Almqvist and E. Stenlund, Comput. Phys. Commun. **43**, 387 (1987); B. Andersson, G. Gustafson, and B. Nilsson-Almqvist, Nucl. Phys. **B281**, 289 (1987).

²⁰Although Boltzmann fits were used for Fig. 3 in Ref. 1, exponential fits have been used to obtain all rapidity distributions in this paper. The difference is negligible for kaons and protons and roughly (10-15)% for pions.

²¹E814 Collaboration, J. Barrette *et al.*, Phys. Rev. Lett. **64**, 1219 (1990).

²²The K^+/π^+ ratios obtained at $1.2 \leq y \leq 1.4$ in $p+Be$, $p+Au$, and central Si+Au collisions are $(7.8 \pm 0.4)\%$, $(12.5 \pm 0.6)\%$, and $(18.2 \pm 0.9)\%$, while K^-/π^- ratios are $(2.0 \pm 0.2)\%$, $(2.8 \pm 0.3)\%$, and $(3.2 \pm 0.3)\%$, respectively. Note that the K/π ratios quoted in Ref. 1 were the average of the results obtained using the exponential and Boltzmann fits and, unlike this work, include an estimate of systematic uncertainty.